8.A.8 Nuclear Physics B18 (1970) 425-458. North-Holland Publishing Company

THE $\bar{K}N$ INTERACTION FROM 800 TO 1200 MeV/c (IV). CROSS SECTIONS OF K^-n REACTIONS

R. ARMENTEROS, P. BAILLON, P. LEXA‡, A. MINTEN, K. H. NGUYEN ⌗, E. PAGIOLA and V. PELOSI⌗⌗
CERN, Geneva

R. BARLOUTAUD, F. BIGATA, M. CROZON *, C. LOUEDEC, J. L. NARJOUX * and F. PIERRE
CEN, Saclay

Received 8 January 1970
(Revised 22 January 1970)

Abstract: K^--neutron reactions have been studied at eight different K^- momenta between 700 and 1175 MeV/c. Taking into account the Fermi motion of the neutron in the deuteron, this momentum range corresponds to a mass range of the K^-n system between 1600 and 1900 MeV. 200 000 photographs with about 8 tracks/picture were taken in the 81 cm Saclay bubble chamber, filled with deuterium and exposed to a separated K^- beam at the CERN proton synchrotron. A total of about 34 000 events has been obtained. Analysis and cross sections of the main reactions are reported.

1. INTRODUCTION

This experiment is part of a comprehensive study of the K^- nucleon interaction around 1 GeV/c. The results of the first part, which consisted of a hydrogen bubble chamber exposure at 23 different momenta from 777 to 1226 MeV/c, have already been reported in this series [1].

This report deals with an exposure in deuterium at eight momenta: 702, 778, 837, 903, 964, 1034, 1098 and 1173 MeV/c. The exposure took place in a separated K^- beam at the CERN proton synchrotron [2]. All momenta except the lowest were selected by tuning the beam magnets. The momentum of 702 MeV/c was obtained by degrading the energy of 800 MeV/c kaons by means of a copper absorber in front of the entrance window of the bubble chamber. 200 000 photographs with about 8 tracks/picture were taken in the Saclay 81 cm bubble chamber filled with deuterium; the magnetic field in the chamber center was 20.74 kG.

‡ Institut für Hochenergiephysik, Heidelberg.
⌗ Institut de Physique Nucléaire, Faculté des Sciences, Paris.
⌗⌗ University of Milan.
* Collège de France, Laboratoire de Physique Atomique, Paris.

The purpose of the experiment is to study the isospin $I = 1$ part of the K^- nucleon interaction. This is of special interest in the field of hyperon resonances such as $Y_1^*(1760)$ and $Y_1^*(1660)$ both of which are in the region of isospin $I = 0$ resonances, namely $Y_0^*(1820)$ and $Y_0^*(1690)$, whose amplitudes interfere in the K^-p channel with the $I = 1$ waves. Partial investigations of the problem have already been reported earlier by other laboratories [3] and the CERN-Heidelberg-Saclay collaboration [4]. Here we present a general treatment of the deuterium analysis and give the cross sections of the different reactions. The paper is separated into: (i) description of the special scanning and fitting procedure of K^-n interactions; (ii) presentation of partial cross sections as function of the c.m. energy of the K^-n system, or the equivalent incident K^- momentum on a free nucleon; and (iii) tabulation of the differential cross sections for the predominant two-body final states K^-d, K^-n, $\Lambda\pi^-$, $\Sigma^0\pi^-$ and $\Sigma^-\pi^0$, and the polarisation of the Λ in the $\Lambda\pi^-$ state.

2. EXPERIMENTAL PROCEDURE

2. 1. *Scanning*. The event selection on the scanning table was established to choose interactions which are either clear or possible interactions of the K^- with the neutron in the deuteron. This procedure is based on the impulse approximation, which assumes that an incident particle, in first order, interacts with *one* of the nucleons in the deuteron, and the second nucleon is considered as spectator. The momentum distribution of this unaffected spectator nucleon is described by the deuteron wave function. Therefore we conclude that reactions on the neutron are characterized by the presence of a low-energy proton, and consequently an event was selected as a possible K^-n reaction if it met one of the following criteria:

(a) It had an *odd* number of outgoing tracks with total negative charge. The spectator proton was assumed to be invisible because its momentum was smaller than 80 MeV/c and thus could not produce a detectable track in liquid deuterium;

(b) It had an even number of outgoing tracks with total charge zero and one of the (positive) secondaries could be identified as a proton stopping inside the bubble chamber with a projected range smaller than 12 cm, corresponding to a momentum of about 250 MeV/c.

For reactions with two nucleons in the final state as for example

$$K^-d \rightarrow pnK^- \,, \tag{2a}$$

$$K^-d \rightarrow ppK^-\pi^- \,, \tag{2e}$$

there is an ambiguity as to which of the two nucleons in the deuteron was the target particle. For these event types the ambiguity was reduced on the basis of the probability distribution of the spectator momentum as given by the deuteron wave function. For *inelastic* reactions such as (2e) above the difference in the momenta of the two nucleons is generally large, and furthermore the nucleon with the lower momentum falls normally well within

Table 1
Event topologies and corresponding reactions.

Topology	Reactions	No. of events
1 prong A 2 prong S	$K^-d \to dK^-$, pK^-n, pK^-M, $p\pi^-$ (Λ, Σ^0), $p\pi^-\bar{K}^0n$	20643
3 prong τ	$K^- \to \pi^-\pi^+\pi^-$	2705
3 prong 4 prong S	$K^-d \to p\,pK^-\pi^-$, $p\pi^+\pi^-\pi^-(\Lambda^0, \Sigma^0)$	815
1 prong + V^0 2 prong S + V^0	$K^-d \to p\,\pi^-\bar{K}^0n$ $p\,\pi^-\Lambda^0$, $p\,\pi^-\Sigma^0$, $p\,\pi^-\Lambda^0\pi^0$	545 5775
3 prong + V^0 4 prong S + V^0	$K^-d \to p\,\pi^+\pi^-\pi^-\Lambda^0$, $p\,\pi^+\pi^-\pi^-\Sigma^0$	161
1 prong + V^- 2 prong S + V^-	$K^-d \to p\,K^-n$, $p\,\Sigma^-\pi^0$, $p\,\Sigma^-M$	2390
3 prong + $V^\pm$ 4 prong S + $V^\pm$	$K^-d \to p\,pK^-\pi^-$, $p\,\Sigma^\pm\pi^\mp\pi^-$, $p\,\Sigma^\pm\pi^\mp\pi^-\pi^0$	1133
	Total:	34167

A "arrière", secondary going backwards in the laboratory.
S "spectator proton", positive track $\leqslant$ 12 cm, stopping in the bubble chamber, heavily ionizing.
V^0 decay of a neutral strange particle, e.g. $\bar{K}^0 \to \pi^+\pi^-$, $\Lambda \to p\pi^-$.
$V^\pm$ decay of a charged strange particle, e.g. $K^- \to \pi^-\pi^0$, $\Sigma^+ \to p\pi^-$, π^+n, $\Sigma^- \to \pi^-n$.
M multineutral system.

the range given by the Fermi motion of the spectator. So there is little difficulty in separating target and spectator. *Elastic* scattering, reaction (2a), on the contrary, occurs predominantly at small momentum transfers and the ambiguity cannot be resolved in most of the cases.

The selected topologies together with the possible contributing reactions are listed in table 1. The letter S (spectator) with an even prong reaction indicates that a positive track stops in the bubble chamber, has a projected range of less than 12 cm and is heavily ionising. The letter M indicates that no fit with a single neutral particle was possible. The film was scanned twice and the scanning efficiency, obtained by calculation from the comparison of the two scans, was close to 100%. This does not take into account the special scanning biases for the individual topologies, such as the azimuthal distribution of short spectator protons, which escape detection if they dip steeply. As it will be discussed later, such effects were corrected for by proper cuts and weights.

2.2. *Data treatment*

After measurement by film plane digitizing machines, the events were passed through the conventional CERN program chain THRESH-GRIND-SLICE-SUMX.

Before the kinematic fit of an event, the momentum of the incoming K^- was beam-averaged. For this reason all τ-decays ($K^- \to \pi^+\pi^-\pi^-$) were

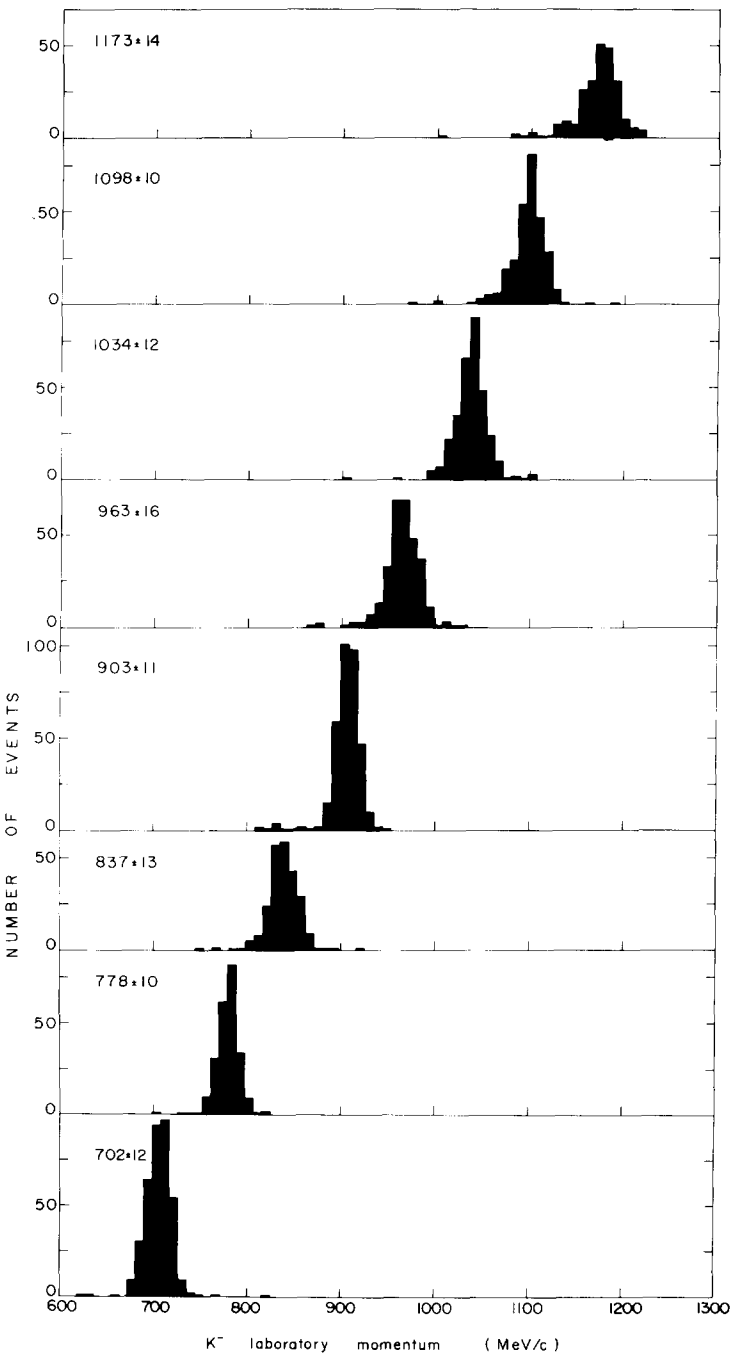

Fig. 1. Momentum distributions of the incident K^- mesons as obtained from τ decays $K^- \rightarrow \pi^-\pi^+\pi^-$; numbers indicate mean value and rms width of the distributions in MeV/c.

measured and fitted. The K^- momenta obtained after the fit were used to obtain the average beam momentum and its error, $< p_T > \pm \sigma_T$, at a well-defined point in the bubble chamber. The values of these quantities are given, together with the distributions, in fig. 1. Before fitting an interaction the measured momentum of the K^- and its error $p_K \pm \sigma_K$ and the mean quantities $< p_T > \pm \sigma_T$, transformed to the interaction point, were combined to a weighted average and used as starting values for the fit.

Events which failed in the reconstruction were reexamined on the scanning table and remeasured. Ambiguities, if solvable by ionisation criteria, were decided at the same stage. Unmeasurable events were apportioned to the corresponding reactions proportionally to the number of accepted events. Thus the rejected events are accounted for in the cross-section calculations.

In general, a fit was considered acceptable if its confidence level was better than 1%. Events containing the decay of a strange particle such as K^0, Λ, $\Sigma^\pm$ were processed by a three step procedure:

(a) reconstruction of the strange particle by a fit at the decay vertex;

(b) with the result of (a) a fit at the production vertex was tried;

(c) if (a) and (b) were successful, a multivertex fit using all measured quantities was performed. Only events with a successful multivertex fit were accepted for further analysis of two-body reactions. For the study of some reactions with several neutrals such as

$$K^-d \rightarrow p\Sigma^- + \text{neutrals} ,$$

no fit is possible, but the missing mass calculation allowed a unique classification, as, for example, in the case

$$K^-d \rightarrow p\Sigma^-\eta \quad \text{with} \quad \eta \rightarrow \text{neutrals} .$$

In the statistical treatment of the sample two main corrections were made:

(a) Correction of decay losses for strange particles as $\bar{K}^0$, Λ, $\Sigma^\pm$. Losses occur if the strange particle decays close to its production vertex, where it may escape detection, or if the decay occurs outside the bubble chamber. To correct these effects, a shortest projected decay length $l_0 = 3.5$ mm is defined; events with $l < l_0$ are rejected, and all others are weighted by a factor $W > 1$

$$W = (\exp(-l_0/L \cos\lambda) - \exp(-l_p/L))^{-1} ,$$

where L is the decay length of the strange particle, λ the dip angle, and l_p the potential length, i.e. the longest possible detectable pathlength of the individual event in the fiducial volume of the bubble chamber.

(b) Correction for scanning inefficiencies for certain geometrical configurations. This is, for example, the case for Σ-decays in which the charged decay particle makes a very small angle with the Σ-track. A similar loss occurs for two prongs, when the secondary direction coincides with the direction of the spectator proton. Both effects depend strongly on

the dip angle of the track in question. On these a correction was made by cutting out the events in the affected angle region, and by weighting the remainder by a weight, based on isotropy of the decay particles in the Σ rest system in the first case, or on the isotropy of the spectator protons in the lab in the second case.

2.3. *Treatment of spectator protons*

The kinematic fit to reactions on a deuteron target can be performed in the standard way, if the spectator proton is visible. A special method, however, has to be applied for events with invisible spectators. The conventional procedure would in this case consider the proton as unmeasured and obtain its momentum vector by a fit. Thereby three kinematic constraints would be used up and would not allow the fit of an additional neutral particle, e.g. the reaction

$$K^- d \rightarrow p_S \Lambda \pi^- \pi^0 \tag{3b}$$

could not be fitted if p_S was invisible. To avoid this consequence, the fact that the unseen proton has a range of $\cdot$ 1 mm and thereby a momentum of $\cdot$ 80 MeV/c was used in the following procedure: for events with an odd number of prongs (for three prongs only if the τ hypothesis failed) a zero length "measured" proton was added with its momentum vector defined by: $p_x = p_y = p_z = 0$; $\Delta p_x = \Delta p_y = \pm$ 30 MeV/c, $\Delta p_z = \pm$ 40 MeV/c, where z is the direction of the camera axis and the increased value of Δp_z accounts for the lower detection probability along z. The fit for the invisible spectator was performed in Cartesian coordinates in order to avoid the singularity for $|p| = 0$.

Fig. 2 shows the fitted spectator momentum for the four- and one-constraint reactions

$$K^- d \rightarrow p_S \Lambda \pi^- , \tag{3a}$$

$$\rightarrow p_S \Lambda \pi^- \pi^0 . \tag{3b}$$

It can be seen, that for the four-constraint fit of the reaction (3a) the experimental distribution for visible and invisible spectator protons agree well with curves calculated from the Hulthén distribution [5, 6]. This distribution is simulated at low momenta by a Gaussian curve with $p_x = p_y = p_z = 0$ and standard deviations of $\Delta p_x = \Delta p_y = 30$ MeV/c, $\Delta p_z = 40$ MeV/c (fig. 2a).

A clear disagreement (fig. 2b) occurs in the one-constraint fit of reaction (3b). Here the fitting procedure leaves the starting values essentially unchanged for invisible spectators, so that the true distribution is not reproduced. Therefore the fitted momentum values of the unseen particles (in this reaction the proton and the neutral pion) are biased.

2.4. *Analysis of the reaction $K^- d \rightarrow pnK^-$*

We consider the analysis of elastic and quasi elastic scattering of a K^- meson on a deuteron, namely the reactions:

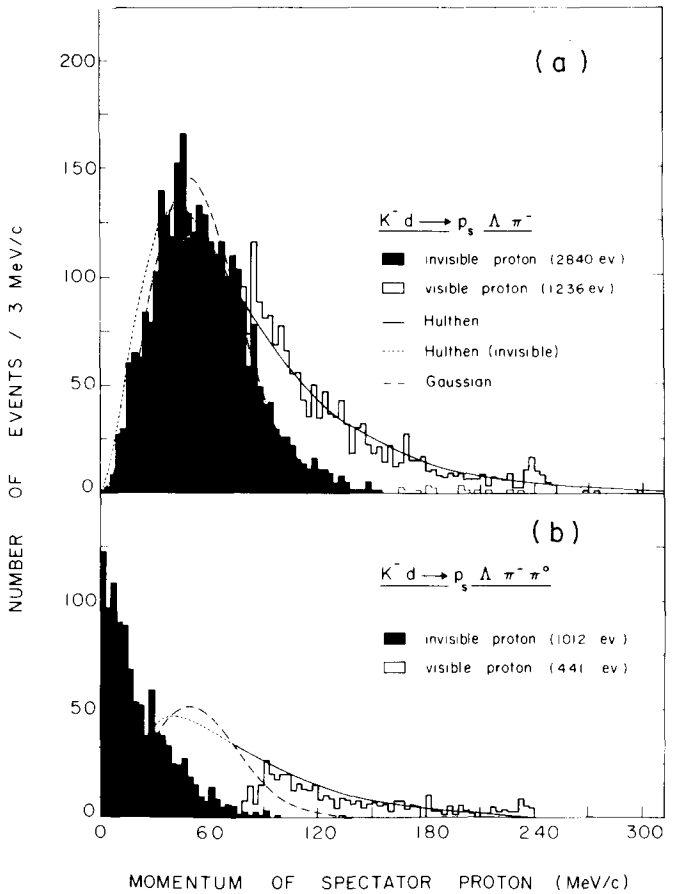

Fig. 2. Experimental histograms and calculated curves of the momentum distribution of the spectator proton in a K^-d reaction. Shaded areas represent invisible, clear areas visible spectators. The solid and dashed curves give the distributions as predicted from Hulthen theory, where the dashed part contains the additional condition of a projected proton range of less then 1 mm. The dash-dotted curve was obtained by reproducing a random distribution with the kinematic constraints:
$p_x = p_y = p_z/1.37 = (0 \pm 30)$ MeV/c
(a) reaction $K^-d \rightarrow p_S \Lambda \pi^-$ (4 constraints), (b) reaction $K^-d \rightarrow p_S \Lambda \pi^- \pi^0$ (1 constraint).

$$K^-d \rightarrow dK^- , \tag{1}$$

$$K^-d \rightarrow pnK^- . \tag{2a}$$

Whereas reaction (1) clearly corresponds to a well defined physical process, where the deuteron recoils as a whole, reaction (2) cannot be attributed unambigously to the scattering of the K^- on the neutron

$$K^-d \rightarrow p_S nK^-$$

Reactions (1) and (2) occur topologically as one-prong and two-prong events.

Of these, the one-prong events are strongly contaminated by K^- decays and were generally not accepted on the scanning table. Nevertheless, in order to increase the statistical accuracy in the determination of the differential cross section for reaction (2b), one-prong events were also accepted, if the secondary was found to go backwards in the lab. In this case the scattered K^- could be distinguished by ionisation from π^- or μ^- resulting from K^- decays. The backward scattering events were then added to the sample of events with visible spectators, applying a normalization procedure that will be described later (sect. 3).

Another possible contamination to reaction (2a) arises from events fitting both reactions (2a) and (3a).

$$K^-d \rightarrow p\pi^-\Lambda \quad \Lambda \rightarrow n\pi^0 \,. \tag{3a}$$

One can discriminate between pion and kaon by means of ionisation criteria up to a momentum of 600 MeV/c. At higher meson momenta ambigous events were retained. To determine this contamination, a fit to reaction (2a) was tried for the events fitting reaction (3a) with a *visible* Λ-decay ignoring the information from the visible lambda. The number of successful fits thus obtained was subtracted from the sample of events attributed to reaction (2a), with a weight taking into account the probability of not observing the decay of the Λ.

The two-prong topology was further restricted by the general requirement that the positive track has a projected length smaller than 12 cm, be heavily ionizing and stop in the bubble chamber. Physically this cut implies a reduction of the sample in favour of reaction (2b), where the proton is a spectator. This cut also affects events from reaction (1) where it cancels the region of momentum transfer ≥ 0.3 $(\mathrm{GeV}/c)^2$.

The two-prong events are subject to the following detection inefficiencies:

(i) The length of the proton (deuteron) track. A minimum projected length of 1 mm was required on the scanning table. But when looking at the distribution of this length for all scanned two-prong events, we clearly observe a loss of events between 1 and 2 mm. To reduce this effect, protons and deuterons with a dip angle of more than one radian were eliminated from the analysis.

In order to correct for the losses of events with a projected length between 1 and 2 mm, we have determined a detection efficiency and a weight for each event. This detection efficiency was calculated assuming that it depends only on the projected length of the proton (deuteron) and using the expected symmetry of the reaction around the incident K^-. We therefore selected a sample of events with a proton (deuteron) of more than 3 mm range in space and an angle between the normal of the (K^-_{inc}, proton) plane and the optical axis less than 30^o. This means a projected length bigger than 2.5 mm. Rotating randomly the events of this sample around the directions of the incident K^-, a distribution of projected lengths for proton (deuterons) with a range bigger than 3 mm in space was generated. Comparing

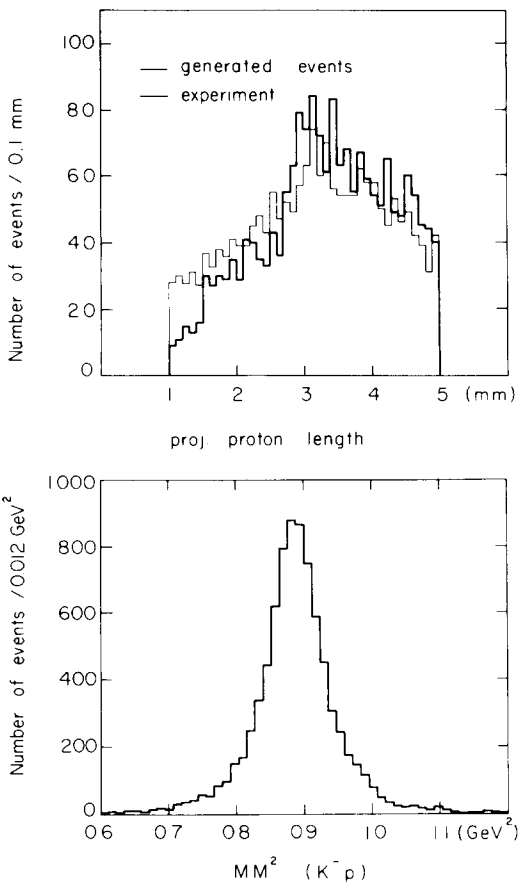

Fig. 3. Reaction $K^-d \rightarrow K^-pn$. (a) Distribution of events versus the projected length of the stopping proton. Events were generated by rotating a sample with a small dip angle. (b) Square of the missing mass to the (K^-p) system. Elastic events were accepted for $0.76 \leq MM^2 \leq 1.0$ GeV^2.

it with the experimental one, we can determine the detection efficiency and the corresponding weight as a function of the projected length (fig. 3a).

Further inefficiencies were caused by:

(ii) The superposition of the incident or scattered K^- and the spectator proton in reaction (2b).

(iii) The collinearity of the incident and scattered K^- in reaction (2b).

The two last effects were corrected for by introducing cuts in the angles between the direction of the incident K^- and the direction of spectator, or outgoing K^-, respectively. The cut region was compensated for by geometrical weight factors, obtained by a Monte-Carlo calculation taking into account the deuteron wave function.

The remaining problems are the separation of reactions (1), (2a) and (2d)

$$K^-d \to pnK^-\pi^0 , \tag{2d}$$

and the separation of (2b) and (2c), namely

$$K^-d \to p_S nK^- , \tag{2b}$$

$$K^-d \to n_S pK^- . \tag{2c}$$

Events of reaction (1) are extracted by a four-constraint fit from the measured quantities. Obviously, there are always events from reaction (2a) which accidentally fulfill the kinematical condition for (1). Their proportion was minimized by appropriate cuts in the missing momentum and the missing mass to the deuteron in reaction (1). The separation between reactions (2a) and (2d) was achieved by a cut in the square of the missing mass to the K^-p system at 1 GeV^2 (fig. 3b).

After these cuts the contaminations in reactions (1) and (2a) are estimated to be below the 1% level. Corrections for the different cuts were applied in the final cross-section calculation (subsect. 3.2).

Events of reaction (2a) can, in the frame of the impulse approximation, belong either to reaction (2b) or (2c), and there is no way of separating them by *kinematic* arguments. On the other hand, the deuteron wave function provides, as it is shown immediately below, a way of separating (2b) and (2c) by arguments of *probability*.

Let p_p be the momentum of the proton in the deuteron, $\psi_d(p_p)$ its wave function in momentum space, and $\phi_n(m_{K^-n}, \theta^*_{K^-n})$ the amplitude at a c.m. energy m_{K^-n} of an incident K^- scattering on the neutron by a c.m. angle $\theta^*_{K^-n}$. Then the total amplitude is

$$\Phi_n(p_p, m_{K^-n}, \theta^*_{K^-n}) = \psi_d(p_p)\phi_n(m_{K^-n}, \theta^*_{K^-n}) .$$

Adding an equivalent term for K^-p scattering we obtain

$$\Phi = \psi_d(p_p)\phi_n(m_{K^-n}, \theta^*_{K^-n}) + \psi_d(p_n)\phi_p(m_{K^-p}, \theta^*_{K^-p}) ,$$

$$|\Phi|^2 = |\psi_d(p_p)|^2|\phi_n|^2 + |\psi_d(p_n)|^2|\phi_p|^2 + 2\,\mathrm{Re}\,\psi_d(p_n)\psi^*_d(p_p)\,\phi_p\,\phi^*_n .$$

All quantities p_n, p_p, m_{K^-p}, $\theta^*_{K^-p}$, $\theta^*_{K^-n}$ are known. We now define as interactions on the neutron those events with a probability for the neutron being a spectator

$$\frac{p_n^2|\psi_d(p_n)|^2}{p_p^2|\psi_d(p_p)|^2 + p_n^2|\psi_d(p_n)|^2} < 0.02 ,$$

where the factor p^2 represents the volume element in phase space. The region eliminated by this condition contains the scattering up to angles with $\cos\theta^*_{K^-n} \approx 0.6$. It was accounted for (as well as the other cuts due to scanning biases (i) to (iii)) in the final Monte-Carlo calculation (see subsect. 3.2).

The expression

$$|\psi_d(p_n)|^2|\psi\ |^2 + 2\ \mathrm{Re}\ \psi_d(p_n)\psi_d^*(p_p)\ \phi_p\ \phi_n^* ,$$

contains the scattering on the proton. It is dominated by the interference term, which would be of the order of 28% of the main term in the extreme case, when Φ_p and Φ_n are exactly in phase. This case is unlikely to be true in the remaining angular region. Assuming a fast phase variation of Φ_p with the variables m_{K^-p} and $\theta^*_{K^-p}$, we expect the interference term to be much smaller.

2.5. *Analysis of the reactions* $K^-d \to p\Lambda\pi + neutrals$

In this chapter we describe the treatment of the topologies: one-prong plus V^0 and two-prongs plus V^0. We do not discuss here the reaction with a $\bar{K}^0$ in the final state

$$K^-d \to pn\bar{K}^0\pi^- \tag{3e}$$

because it does not create any special problems. The observation of a Λ decay leads to one of the following reactions:

$$K^-d \to p\Lambda\pi^- \tag{3a}$$

$$p\Lambda\pi^-\pi^0 \tag{3b}$$

$$p\Lambda\pi^- M \tag{3c}$$

$$p\Sigma^0\pi^- \tag{4a}$$

$$p\Sigma^0\pi^-\pi^0 \tag{4b}$$

$$p\Sigma^0\pi^- M , \tag{4c}$$

where M represents a multi-neutral system. The combined contributions of reactions (3a) and (4a) can be easily separated from the other reactions by a cut in the missing mass, MM, to the $p\pi^-$ system (fig. 4a). In the region up to $MM^2 \approx 1.6\ \mathrm{GeV}^2$ we observe the Λ and Σ^0 masses clearly separated from the high-mass region beyond 1.6 GeV^2, probably consisting of resonances such as:

$$Y_1^*(1385) \to \Lambda\pi^0 ,$$

$$Y_0^*(1405) \to \Sigma^0\pi^0 ,$$

$$Y_0^*(1520) \to \Sigma^0\pi^0 .$$

We now concentrate on the separation of the $\Lambda\pi^-$ and $\Sigma^0\pi^-$ final states. To do this we consider the events with a missing mass $MM^2(p\pi^-) \cdot 1.55\ \mathrm{GeV}^2$, (figs. 4a and 4b) and we assume, for the moment, that they all belong to reaction (4a), namely the $\Sigma^0\pi^-$ final state. With this assumption we then calculate, from the measured quantities, the angle between the directions of the Σ^0 and its decay γ in the Σ^0 rest system:

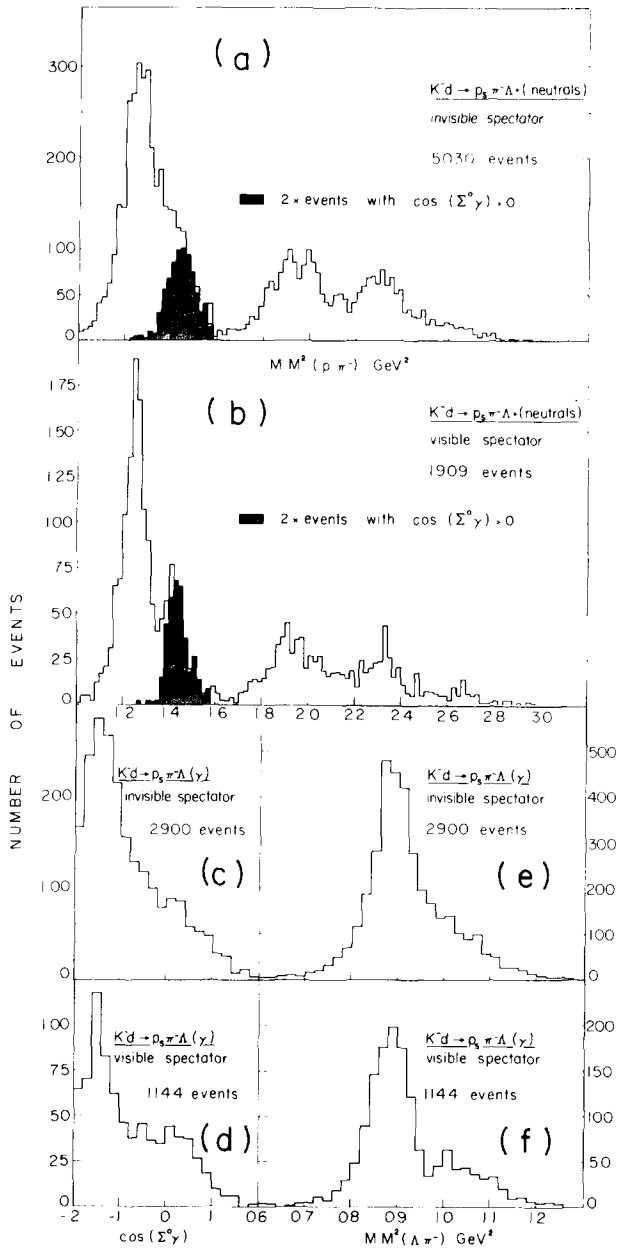

Fig. 4. (a) Distribution of the square of the missing mass to the $p\pi^-$ system in the reaction $K^-d \rightarrow p_S \Lambda\pi^-$ (+ neutrals) for invisible spectator protons. The shaded area contains events fitting the $p_S\Sigma^O\pi^-$ final state; (b) the same as (a) for visible spectators only; (c) cosine of the angle between the (assumed) Σ^O and the decay γ for all events of the reaction $K^-d \rightarrow p_S\Lambda\pi^-$ (+ neutrals) with $MM^2(p\pi^-) < 1.57$ GeV^2 for invisible spectators only; (d) same as (c), visible spectators only. The area with cos $(\Sigma^O\gamma) > 0$ represents events of the reaction $K^-d \rightarrow p_S\Sigma^O\pi^-$, whereas the peak at the unphysical angles cos $(\Sigma^O\gamma) < -1$ contains the $\Lambda\pi^-$ final state; (e) distribution of the square of the missing mass to the $\Lambda\pi^-$ system; a symmetric region around the proton mass contains the $p_S\Lambda\pi^-$ final state, higher masses represent the effective $(p_S\gamma)$ mass of the $p_S\Sigma^O\pi^-$ states; invisible spectators only; (f) same as (e), visible spectators only.

$$\cos(\Sigma^0\gamma) = \left[\frac{(2M_\Sigma^2 E_\gamma^{lab})}{E_\Sigma^{lab}(M_\Sigma^2 - M_\Lambda^2)} - 1\right] \frac{E_\Sigma^{lab}}{p_\Sigma^{lab}}.$$

Here Σ^{lab} is the missing energy to the $(p\pi^-)$ system, p_Σ^{lab} the corresponding momentum and E_γ^{lab} is the missing energy to the $(p\pi^-\Lambda)$ system.

The $\Lambda\pi^-$ events which were wrongly assumed to be a $\Sigma^0\pi^-$ final state, will tend to give $E_\gamma^{lab} \approx 0.$, i.e. the quantity $\cos(\Sigma^0\gamma)$ will go to the unphysical value (fig. 4c, d)

$$\cos(\Sigma^0\gamma) \to -1 .$$

In order to obtain: (a) a pure sample of Σ^0 events, (b) the relative number of Λ^0 and Σ^0 events, (c) a pure sample of Λ^0 events we proceeded as follows:

(a) Events with $\cos(\Sigma^0\gamma) > 0$ are considered to constitute a pure sample of the $p\Sigma^0\pi^-$ reaction.

(b) Assuming a flat distribution in $\cos(\Sigma^0\gamma)$, we multiply the number of events with $\cos(\Sigma^0\gamma) > 0$ by two. The result is considered as the total number of Σ^0 events, the remainder as the total number of Λ^0 events. This procedure can be checked going back to figs. 4a and b where twice the number of events with $\cos(\Sigma^0\gamma) > 0$ are shown with their missing mass squared to the $p\pi^-$ system. We observe that the Σ^0 peak is reproduced.

(c) To find a pure sample of $p\Lambda\pi^-$ events, we have to apply different methods for events with visible and invisible spectators. In the first case a cut in the missing mass squared to the $p\pi^-$ system at 1.35 GeV^2 provides a sufficiently good separation. For events with an invisible spectator proton we consider the missing mass to the $\Lambda\pi^-$, which is the mass of the $p\gamma$ system (figs. 4e, f). We find an asymmetric distribution, in which the higher $p\gamma$ masses represent the $p\Sigma^0\pi^-$ final state. We further (i) require a 1% confidence level for the $p\Lambda\pi^-$ hypothesis, (ii) cut the distribution at $M^2(p\gamma) = 1.08$ GeV^2. The remaining contamination of $\Sigma^0\pi^-$ events in the $\Lambda\pi^-$ sample was subtracted.

The number of these events, roughly 10%, was obtained from (b). This number of events was removed, separately at each incident momentum, in the differential cross section by using the angular distribution of the reaction $K^-d \to p_S\Sigma^-\pi^0$.

We now concentrate on the evaluation of the cross section of the reaction

$$K^-d \to p\Lambda\pi^-\pi^0 . \qquad (3b)$$

This reaction can be easily separated from those with a three-body final state, (3a) and (4a), by a cut at 1.6 GeV^2 in the missing mass to the $(p\pi^-)$ system (figs. 4a, b). On the other hand, reaction (3b) is in general ambiguous with four-body final states, namely (3c), (4b) and (4c). In order to separate (3b), we used the fact that the $(\pi^-\pi^0)$ system is a pure isospin $I = 1$ state, and must therefore have an antisymmetric wave function. This implies that the scatter plot of $M^2(\Lambda\pi^-)$ versus $M^2(\Lambda\pi^0)$ has to be symmet-

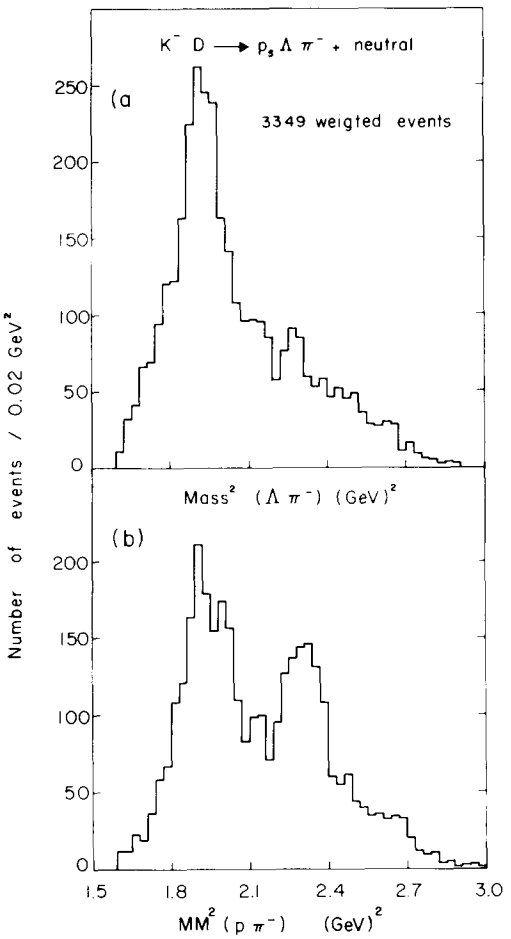

Fig. 5. (a) Square of the effective mass of the $(\Lambda\pi)$ system in the reaction $K^-d \rightarrow p\Lambda\pi^- +$neutrals; (b) square of the missing mass to the $(p\pi^-)$ system in the same reaction.

ric with respect to the diagonal. Fig. 5 shows the projections of this plot for *all* four body events, where $M^2(\Lambda\pi^0)$ is replaced by $MM^2(p\pi^-)$, which are equivalent for the $p\Lambda\pi^-\pi^0$ state. A difference can only be seen in the Y_0^* (1520) region. A similar observation is made if only events with a good fit to reaction (3b) are retained. From that we infer that the reactions (3c, 4b, 4c) contribute mainly in this region, probably by $Y^*(1520) \rightarrow \Sigma^0\pi^0$. So we eliminate the region $2.18 \leqslant MM^2(p\pi^-) \leqslant 2.4$ GeV^2 and replace it by events in the equivalent region with $2.18 \leqslant M^2(\Lambda\pi^-) \leqslant 2.4$ GeV^2, using the symmetry property mentioned above. A possible contamination from $Y^*(1405) \rightarrow \Sigma^0\pi^0$ was estimated to be small.

2.6. *Analysis of the reaction* $K^-d \to p\Sigma^- + neutral(s)$

We consider the following reactions:

$$K^-d \to p_S\Sigma^-\pi^0 , \tag{5a}$$

$$\to p_S\Sigma^-\pi^0\pi^0 , \tag{5b}$$

$$\to p_S\Sigma^-\eta \quad \Big\lfloor \to \text{neutrals} , \tag{5c}$$

with the Σ^- decaying via

$$\Sigma^- \to n\pi^- . \tag{6}$$

Reactions (5a) to (5c) are defined topologically by a one-prong event, where the negative track shows a decay, or a two-prong event where the negative decaying particle is accompanied by a spectator proton. The detection of these events suffers from three scanning biases (fig. 6):

(i) if the laboratory production angle of the Σ^- is small, a loss of events is observed, preferentially if the spectator proton is invisible. In order to correct for this bias a cut was applied at a lab projected angle of 5^0. Accepted events were weighted assuming isotropy of the Σ^- production around the incident K^-. The resulting distribution was then extrapolated to

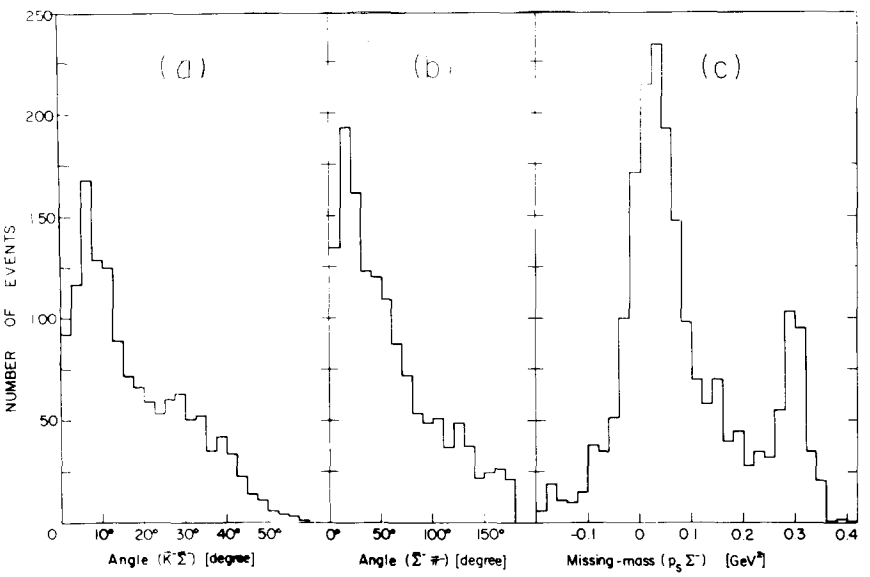

Fig. 6. Study the reaction $K^-d \to p_S\Sigma^-$ + neutrals; (a) distribution of the projected lab Σ^- production angle with respect to the incoming K^-. The dip at $\approx 0^0$ is interpreted as a detection bias; (b) distribution of the projected lab Σ^- decay angle of the π^- with respect to the Σ^- direction. A detection loss in observed for 0^0 decays; (c) distribution of the square of the missing mass to the $(p_S\Sigma^-)$ system. The enhancements belong to the $p_S\Sigma^-\pi^0$ and $p_S\Sigma^-\eta$ final states.

0^0 to compensate for lost events.

(ii) a loss occurs also if the decay angle of the Σ^- is small. The event would then be classified as a one prong or a two prong, depending on the visibility of the spectator proton. This detection inefficiency was eliminated by ignoring projected decay angles smaller than 5^0 in the laboratory. Since the Σ^- decay angular distribution in the c.m. is isotropic, a weighting factor for the remaining events has been introduced.

(iii) The Σ^- decay can be mistaken with a K^- decay such as

$$K^- \rightarrow \pi^-\pi^0 , \tag{7a}$$

$$\rightarrow \mu^-\nu . \tag{7b}$$

This ambiguity, if not removed by the fit, can normally be solved by checking the ionisation of the Σ^- track. An a posteriori check on the contamination can be obtained from the cross sections of the two-prong reactions

$$K^-d \rightarrow K^-d , \tag{1}$$

$$\rightarrow p_S K^-n . \tag{2b}$$

The number of expected decays from these reactions which can simulate Σ^- events has been found to be equal, within statistics, to the number of ambiguous events in which the Σ^- hypothesis was rejected by the ionisation check.

Another source of confusion is the secondary interaction of a scattered K^- on a neutron without visible spectator. The contamination arising from this double scattering process was estimated from the known cross section for elastic K^-d and K^-n scattering. The resulting number of events was so small that no special correction is necessary.

The number of events attributed to each of the reactions (5a, b, c) was obtained by considering the missing mass to the $p_S\Sigma^-$ system (fig. 6c). This distribution was decomposed into the contributions from the π^0, the η^0 and assuming phase space for the $(2\pi^0)$ events. This procedure is practicable for the combined sample of events, whereas it is statistically limited if applied at each momentum. Therefore the total number of $\Sigma^-\pi^0\pi^0$ events was redistributed to the different momenta proportionally to the available (2π) phase space and the total track length at each momentum.

3. PARTIAL CROSS SECTIONS

3.1. *Cross sections for different momenta*

Cross sections were obtained using τ decays ($K^- \rightarrow \pi^-\pi^+\pi^-$) for normalisation. The cross section is given by the relation

$$\sigma[\text{mb}] = \frac{\text{Number of events}}{\text{Number of taus}} \times \frac{1.7625}{< p_k[\text{GeV}/c] >}$$

The constant 1.7625 is based on a K^- life time of $1.23 \cdot 10^{-8}$ sec., a branching ratio for ($K^- \rightarrow \pi^-\pi^+\pi^-/K^- \rightarrow$ all) = 0.055, and a specific density of

deuterium of 0.140 g·cm^{-3}. The number of events and the number of taus were counted in the same fiducial volume (40 cm in length) in the bubble chamber.

3.2. *Calculation of cross sections*

We assume for the moment that target and spectator nucleon are well defined. In this case there is no interference with the corresponding reaction on the proton. This is not true for a quasi-elastic scattering of the K^- such as $K^-d \rightarrow pnK^-$ where interference effects play an important role.

The analysis of interactions on deuteron targets is based on the *impulse approximation*. In this model proton and neutron are assumed to interact with the incident particle as free particles, but with a momentum distribution described by the deuterium wave function $\psi(\boldsymbol{p})$. We use this so-called Hulthén function [5] in the form given by Moravcsik [6], where $H(\boldsymbol{p}) = |\psi(\boldsymbol{p})|^2$ gives the probability that the proton or neutron moves with a momentum $\boldsymbol{p}$ in the deuteron rest system. Besides the fact that the moving neutron changes the total collision energy E^*, it modifies the flux of the incoming kaons, as we will see below.

The interaction rate dN in the neutron rest system is

$$dN(\boldsymbol{p},\ m^2) = \sigma(m^2)\Phi(\boldsymbol{p})H(\boldsymbol{p})dt\ .$$

Here $\sigma(m^2)$ is the K^-n cross section at the (K^-n) invariant mass m, $\boldsymbol{p}$ is the neutron momentum in the laboratory, $H(\boldsymbol{p})$ is the probability of a neutron having the momentum $\boldsymbol{p}$, and $\Phi(\boldsymbol{p})$ and dt are the K^- flux and the time interval, respectively, both in the neutron rest system, with

$$\Phi = \rho v = \Phi_L\left(\frac{E}{E_L}\frac{v}{v_L}\right)_{\text{kaon}}\ ,$$

$$dt = dt_L\left(\frac{E}{E_L}\right)_{\text{neutron}}\ .$$

Here ρ is the K^- density, v the K^- velocity, and E is the total energy of the K^- or neutron; the quantities indexed with the letter L refer to the lab system, the others to the neutron rest frame. We obtain an interaction rate

$$dN = \Phi_L\sigma\, H(\boldsymbol{p})\left(\frac{E}{E_L}\right)_{\text{neutron}}\left(\frac{E}{E_L}\frac{v}{v_L}\right)_{\text{kaon}} dt_L\ .$$

To obtain the number of events one has to integrate over time and bubble chamber volume

$$N = \sigma\, H(\boldsymbol{p})\left(\frac{E}{E_L}\right)_{\text{neutron}}\left(\frac{E}{E_L}\frac{v}{v_L}\right)_{\text{kaon}}\int \frac{\rho_D}{m_D}\,\phi_L\, dt_L\, dV\ ,$$

where the ratio ρ_D/m_D gives the number of neutrons per cm^3.

Each volume element dV has been chosen to be a cube with one surface perpendicular to the beam. Thus the second integral represents the number of K^- entering the interaction volume times the length of this volume, which is equivalent to the total K^- pathlength, L. So one finds for the total number of interactions:

$$N = \sigma(m^2)\left(\frac{v}{v_L}\frac{E}{E_L}\right)_{\text{kaon}}\left(\frac{E}{E_L}\right)_{\text{neutron}} H(\boldsymbol{p})\frac{\rho_D}{m_D} L .$$

For a given momentum p_K of the incident kaons the length L is related to the observed number of τ decays, N_τ, by

$$L = N_\tau \frac{c\tau p_K}{Bm_K} ,$$

where $B = 0.055$ is the branching fraction of $K^- \to \pi^+\pi^-\pi^-$, τ is the K^- mean lifetime, and c the velocity of light. One finally takes into account the distribution of the neutron Fermi momentum $\boldsymbol{p}$ and the different incident K^- momenta p_K^i.

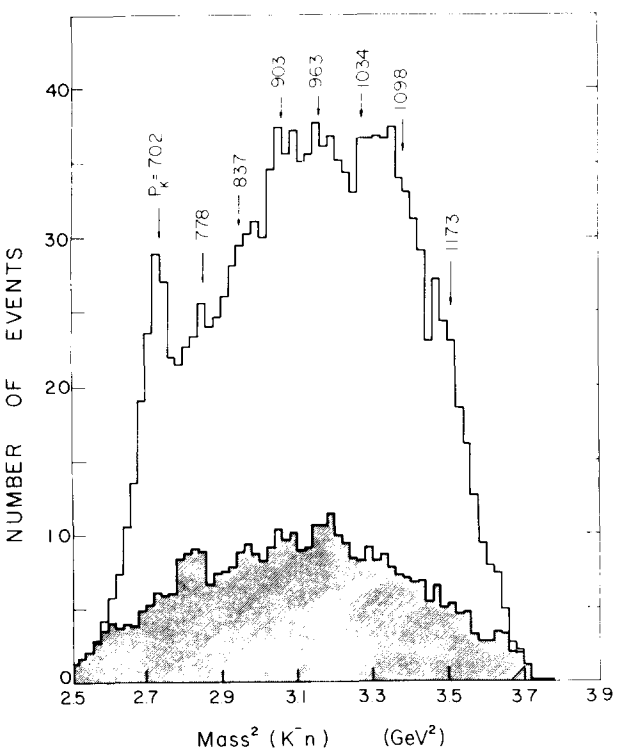

Fig. 7. Number of expected events per mass-squared-bin for a cross section of 1 mb. The histograms are obtained from a Monte-Carlo calculation, taking into account the Fermi motion of the target neutron and the variation of expected yield due to the change in relative motion between K^- and neutron. The latter effect causes also a slight shift of "effective" beam momentum with respect to that on a neutron at rest. The numbers indicate the position for eight nominal beam momenta. The shaded area represents events with visible spectator.

$$N(m^2) = \sigma(m^2)\ \frac{c\tau}{Bm_K}\ \frac{\rho_D}{m_D} \sum_i N_\tau^i \int \left(p_K\ \frac{E}{E_L}\ \frac{v}{v_L}\right)_K^i \left(\frac{E}{E_L}\right)_n H(\boldsymbol{p})\ \mathrm{d}^3\boldsymbol{p}\ .$$

The integration over the Fermi momentum space is performed by means of a Monte-Carlo calculation and the discrete summation over the beam momenta p_K is done using the actual number of τ decays. The result appears as a histogram of the expected number of events per mb cross section versus bins of m^2. In the Monte-Carlo calculation a test on the visibility of the spectator proton according to its projected range was made, and the two categories were recorded separately (fig. 7). The actual experimental cross section was then deduced dividing the number of events found in a particular channel by the number expected for 1 mb.

3.3. *Glauber correction*

According to Glauber [7] the total cross section on a deuteron, σ_D, is related to the cross sections on free nucleons, σ_p and σ_n, by

$$\sigma_D = \sigma_n + \sigma_p - \frac{1}{4\pi}\ \sigma_n\ \sigma_p \langle r_D^{-2} \rangle\ ,$$

where r_D is the deuteron mean radius in the ground state. Here the correction term represents the shadowing of one nucleon by the other, which makes their combined effect smaller than the sum of the bare nucleons. In order to derive the true K^-n cross section $\sigma_R(K^-n)$ from the measured one $\sigma_M(K^-n)$ we assume, that every partial cross section is reduced by the shadowing effect of the proton by the same amount as the total cross section, and we neglect the double scattering effect. So we obtain the *real* cross section

$$\sigma_R(K^-n) = \sigma_M(K^-n)\left(1 - \sigma_{tot}\ (K^-p)\ \langle r_D^{-2} \rangle\ \frac{1}{8\pi}\right)^{-1}\ .$$

We use $\sigma_{tot}\ (K^-p)$ from ref. [8] and $\langle r_D^{-2} \rangle = 0.0423\ \mathrm{mb}^{-1}$.

3.4. *Normalisation with the reaction* $K^-d \rightarrow p_S \Lambda\pi^-$

The cross sections were also normalized to the cross section of the reaction $K^-p \rightarrow \Lambda\pi^0$. This is justified by the fact that this cross section in hydrogen is well known [1] and predicts, by charge independence, the cross section for reaction (5) $K^-n \rightarrow \Lambda\pi^-$ in deuterium. On the basis of the impulse approximation, any cross section for a final state Y is calculated from the relation

$$\sigma(K^-n \rightarrow Y) = 2\sigma(K^-p \rightarrow \Lambda\pi^0)\ \frac{N(K^-n \rightarrow Y)}{1.5\ N(K^-n \rightarrow \Lambda\pi^-)}\ ,$$

where the numbers of weighted events N are taken from the same sample over the same mass interval. For events with an invisible spectator and with a neutral particle in the state Y the calculation of the Y mass is affected with the uncertainty coming from the Fermi motion of the target nucleon. Therefore the mass region covered by the experiment was divided in

eight equal intervals of 30 MeV width centered around the energy corresponding to K^- colliding with a neutron at rest. The width of 30 MeV corresponds approximately to the spread due to the Fermi motion for invisible spectator events. For each interval the number N contains *all* events with invisible spectator from the corresponding momentum and *those* events with *visible* spectator from all momenta, but with the Y or $\Lambda\pi$ mass inside the interval.

The reliability of cross-section calculations in K^-d interactions can be tested by comparing the cross section of the reaction (3a), $\sigma(\Lambda\pi^-)$, as obtained by normalisation with τ decays described above, and the cross section obtained in K^-p collisions [1]

$$K^-p \rightarrow \Lambda\pi^0 .$$

The comparison is made in fig. 8 and indicates cross sections systemati-

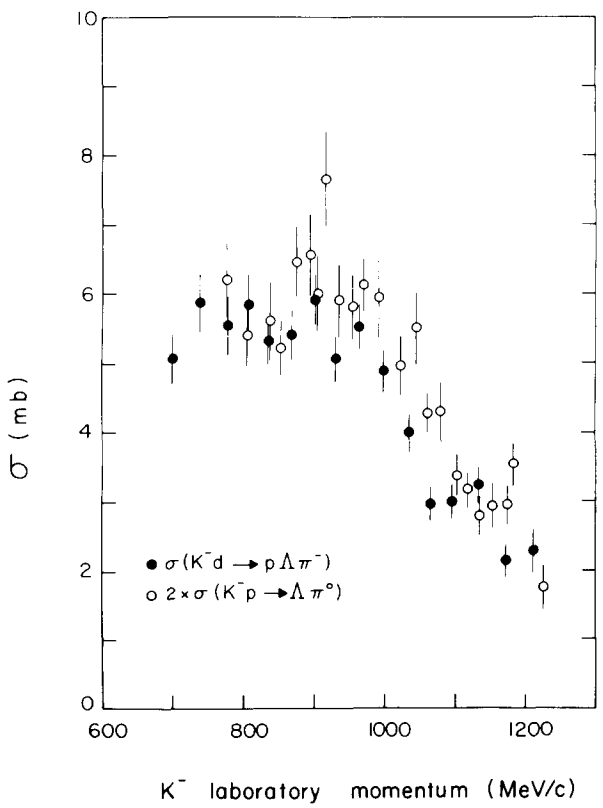

Fig. 8. Cross sections for the reaction $K^-N \rightarrow \Lambda\pi$. Black points are measured in the reaction $K^-d \rightarrow p\Lambda\pi^0$; open points represent twice the cross section measured in hydrogen: $K^-p \rightarrow \Lambda\pi^0$. Charge independence predicts the values to be equal; deviations are probably due to the normalisation in the K^- deuteron reaction.

Table 2
Partial yields for all analysed K^-d reactions at various momenta of the incident K^- on a deuteron at rest.

Reaction \ Momentum (MeV/c)	1 702 ± 12	2 778 ± 10	3 837 ± 13	4 903 ± 11	5 963 ± 16	6 1034 ± 12	7 1098 ± 10	8 1173 ± 14
$K^-d \to K^-d$	7.35 ± 0.30	7.66 ± 0.43	9.04 ± 0.42	8.76 ± 0.36	8.80 ± 0.38	8.59 ± 0.40	7.18 ± 0.36	6.13 ± 0.38
$p_S K^- n$								
$p_S K^- p\pi^-$	0.064 ± 0.02	0.30 ± 0.06	0.61 ± 0.08	0.66 ± 0.07	0.96 ± 0.09	0.74 ± 0.07	0.73 ± 0.07	0.55 ± 0.06
$p_S K^0 \pi^- n$	0.065 ± 0.04	0.31 ± 0.10	0.57 ± 0.12	1.03 ± 0.14	1.59 ± 0.19	1.45 ± 0.17	1.86 ± 0.19	2.12 ± 0.23
$p_S \Lambda^0 \pi^-$	4.46 ± 0.29	5.42 ± 0.35	5.69 ± 0.35	4.47 ± 0.23	4.97 ± 0.24	3.77 ± 0.21	2.93 ± 0.18	2.37 ± 0.18
$p_S \Lambda^0 \pi^- \pi^0$	1.87 ± 0.15	2.44 ± 0.20	3.26 ± 0.22	2.73 ± 0.15	3.03 ± 0.30	2.91 ± 0.15	2.87 ± 0.15	2.25 ± 0.15
a) $p_S \Lambda^0 \pi^-$ neutrals	2.08 ± 0.15	3.02 ± 0.22	4.04 ± 0.22	3.87 ± 0.18	3.95 ± 0.16	3.90 ± 0.16	3.90 ± 0.16	3.24 ± 0.16
$p_S \Lambda^0 \pi^+ \pi^- \pi^-$	0.0 ±	0.09 ± 0.03	0.16 ± 0.04	0.25 ± 0.05	0.24 ± 0.04	0.25 ± 0.05	0.31 ± 0.05	0.24 ± 0.04
$p_S \Sigma^0 \pi^-$	2.16 ± 0.20	1.31 ± 0.18	1.80 ± 0.20	1.20 ± 0.12	1.21 ± 0.12	0.84 ± 0.11	0.95 ± 0.11	0.63 ± 0.09
$p_S \Sigma^- \pi^0$	1.77 ± 0.13	1.68 ± 0.16	1.66 ± 0.16	1.24 ± 0.10	1.17 ± 0.10	0.80 ± 0.08	0.80 ± 0.08	0.61 ± 0.07
$p_S \Sigma^-$ neutrals	0.07 ± 0.03	0.09 ± 0.04	0.24 ± 0.05	0.34 ± 0.05	0.64 ± 0.08	0.53 ± 0.07	0.49 ± 0.06	0.34 ± 0.06
$p_S \Sigma^- \pi^+ \pi^-$	0.24 ± 0.04	0.23 ± 0.05	0.51 ± 0.07	0.50 ± 0.06	0.64 ± 0.08	0.57 ± 0.07	0.52 ± 0.06	0.49 ± 0.06
$p_S \Sigma^+ \pi^- \pi^-$	0.44 ± 0.08	0.48 ± 0.09	0.97 ± 0.12	1.03 ± 0.11	1.33 ± 0.12	1.03 ± 0.10	0.95 ± 0.09	0.73 ± 0.07
$p_S \Sigma^- \pi^+ \pi^- \pi^0$				0.11 ± 0.03	0.21 ± 0.04	0.16 ± 0.03	0.14 ± 0.03	0.12 ± 0.03
								[mb]

a) Includes $\Lambda\pi^-\pi^0$, $\Lambda\pi^-\pi^0\pi^0$, $\Sigma^0\pi^-\pi^0$, $\Sigma^0\pi^-\pi^0\pi^0$.

Normalization with τ decays.

Table 3
Partial cross sections for all analysed K^-d reactions at eight nominal momenta of the incident K^- (normalization with respect to the $\Lambda\pi$ cross section).

Reaction \ Momentum (MeV/c)	702	778	837	903	963	1034	1098	1173
$K^-n \to pK^-\pi^-$	0.30 ± 0.08	0.44 ± 0.10	0.66 ± 0.11	1.12 ± 0.14	1.45 ± 0.15	1.29 ± 0.15	1.08 ± 0.14	0.79 ± 0.13
$nK^o\pi^-$	0.03 ± 0.03	0.39 ± 0.11	0.48 ± 0.16	1.50 ± 0.22	1.80 ± 0.22	2.18 ± 0.26	2.36 ± 0.27	2.83 ± 0.37
$\Lambda\pi^-\pi^o$	2.18 ± 0.29	2.75 ± 0.23	2.99 ± 0.22	3.91 ± 0.28	3.55 ± 0.22	3.95 ± 0.29	3.96 ± 0.28	3.71 ± 0.34
$\Lambda\pi^-$ neutrals	0.34 ± 0.08	0.33 ± 0.07	0.86 ± 0.10	1.24 ± 0.13	1.15 ± 0.11	1.18 ± 0.12	1.19 ± 0.13	0.90 ± 0.13
$\Lambda\pi^+\pi^-\pi^-$	0.02 ± 0.02	0.10 ± 0.04	0.14 ± 0.04	0.24 ± 0.05	0.28 ± 0.05	0.26 ± 0.05	0.37 ± 0.07	0.33 ± 0.07
$\Sigma^o\pi^-$	2.33 ± 0.31	1.74 ± 0.17	1.55 ± 0.15	1.20 ± 0.13	1.18 ± 0.11	1.06 ± 0.12	0.89 ± 0.11	1.00 ± 0.13
$\Sigma^-\pi^o$	2.37 ± 0.30	1.79 ± 0.15	1.65 ± 0.13	1.39 ± 0.12	1.22 ± 0.10	1.11 ± 0.10	0.91 ± 0.10	0.94 ± 0.11
Σ^- neutrals	0.11 ± 0.03	0.09 ± 0.03	0.22 ± 0.04	0.45 ± 0.06	0.74 ± 0.07	0.70 ± 0.08	0.75 ± 0.08	0.49 ± 0.07
$\Sigma^-\pi^+\pi^-$	0.29 ± 0.06	0.30 ± 0.05	0.39 ± 0.06	0.68 ± 0.08	0.86 ± 0.08	0.71 ± 0.08	0.62 ± 0.07	0.53 ± 0.08
$\Sigma^+\pi^-\pi^-$	0.51 ± 0.09	0.55 ± 0.07	0.83 ± 0.09	1.25 ± 0.11	1.57 ± 0.11	1.35 ± 0.12	1.29 ± 0.11	0.93 ± 0.11
$\Sigma^-\pi^+\pi^-[\pi^o]$				0.21 ± 0.05	0.24 ± 0.04	0.24 ± 0.05	0.23 ± 0.05	0.15 ± 0.05
$\Sigma^+\pi^-\pi^-\pi^o$			0.05 ± 0.03	0.06 ± 0.03	0.03 ± 0.02	0.01 ± 0.02	0.06 ± 0.03	0.09 ± 0.04
$K^-n \to \Lambda\pi^-$ a)	5.64 ± 0.60	5.72 ± 0.26	5.34 ± 0.23	5.91 ± 0.30	5.84 ± 0.23	5.16 ± 0.27	3.94 ± 0.19	2.90 ± 0.20
$K^-n \to nK^-\pi^o$ b)	0.01 ± 0.02	0.13 ± 0.08	0.16 ± 0.10	0.50 ± 0.30	0.60 ± 0.36	0.73 ± 0.45	0.79 ± 0.50	0.94 ± 0.50
$\sigma_{reaction}$	14.13 ± 1.60	14.33 ± 0.80	15.32 ± 0.80	19.66 ± 1.10	20.51 ± 0.90	19.93 ± 1.20	18.44 ± 1.00	16.53 ± 1.30 [mb]

a) This cross section which is used to normalize the others, has been obtained from ref. [1] by multiplying the cross section for $K^-p \to \Lambda^o\pi^o$ by two.
b) This cross section was not measured. It was obtained as $(0.33 \pm 0.20)\ \sigma(pnK^o\pi^-)$, assuming that the reaction proceeds via N^*K or NK^*.

Table 4

Partial cross sections for several two-body K^-n reactions at 16 nominal momenta of the incident K^- (normalization with respect to τ-decays).

Reaction \ Momentum	703	739	778	807	837	869	903	932	963	999	1035	1065	1096	1133	1173	1212
$K^-n \rightarrow K^-n$ a)																
$\Lambda\pi^-$	5.06 ±0.36	5.87 ±0.42	5.55 ±0.42	5.83 ±0.44	5.32 ±0.38	5.41 ±0.36	5.91 ±0.35	5.06 ±0.33	5.51 ±0.33	4.88 ±0.30	4.00 ±0.28	2.96 ±0.25	2.99 ±0.24	3.24 ±0.27	2.15 ±0.24	2.29 ±0.31
$\Sigma^0\pi^-$ b)	1.89 ±0.47	2.12 ±0.42	2.38 ±0.46	2.21 ±0.49	1.24 ±0.33	1.54 ±0.36	1.18 ±0.30	1.06 ±0.31	1.27 ±0.29	0.94 ±0.25	1.46 ±0.38	0.90 ±0.30	0.73 ±0.28	1.21 ±0.35	0.63 ±0.28	1.06 ±0.35
$\Sigma^-\pi^0$ b)	2.60 ±0.51	2.25 ±0.40	2.28 ±0.42	2.46 ±0.51	1.25 ±0.32	2.00 ±0.39	0.98 ±0.26	1.15 ±0.29	0.93 ±0.23	1.26 ±0.28	1.13 ±0.28	0.68 ±0.24	1.18 ±0.32	1.06 ±0.29	1.28 ±0.37	0.62 ±0.25

a) The K^-n cross section is given in table 6. It is not reproduced here because it is not obtained purely from the data, but by a fit including the optical point.

b) The $\Sigma^0\pi^0$ cross sections were obtained from events with visible spectator proton only.

Table 5

Differential cross section of the reaction $K^-d \rightarrow K^-d$ at various nominal momenta of the incident K^-.

$2\pi \frac{d\sigma}{d\Omega}$ (mb/sr) $(K^-d \rightarrow K^-d)$

K^- momentum / $\cos\theta$	702	778	837	903	963	1034	1098	1173
opt. point [8]	115.5	137.5	180.0	243.0	285.0	305.0	293.0	259.0
1.0 - 0.98								
0.98 - 0.96	118.3 ± 25.8	113.8 ± 19.8	114.6 ± 15.5	96.2 ± 8.6	105. ± 8.1	76. ± 6.1	61.7 ± 5.1	73.0 ± 6.8
0.96 - 0.94	56.9 ± 5.8	49.3 ± 5.9	74.8 ± 6.7	50.3 ± 4.1	40.7 ± 3.7	59.6 ± 5.4	38.8 ± 3.8	28.3 ± 3.7
0.94 - 0.92	21.9 ± 2.4	30.8 ± 4.0	36.9 ± 4.4	48.2 ± 4.6	39.5 ± 4.0	30.6 ± 3.5	22.2 ± 2.7	13.7 ± 2.4
0.92 - 0.90	18.3 ± 2.6	20.4 ± 3.2	24.3 ± 3.7	20.3 ± 2.6	16.3 ± 2.3	16.6 ± 2.4	15.6 ± 2.3	11.2 ± 2.4
0.90 - 0.88	14.0 ± 2.2	13.6 ± 2.5	15.8 ± 2.7	11.2 ± 2.0	9.8 ± 1.8	14.9 ± 2.7	9.5 ± 1.7	4.1 ± 1.3
0.88 - 0.86	9.9 ± 1.6	14.2 ± 3.0	12.3 ± 2.2	14.9 ± 2.4	5.9 ± 1.4	4.0 ± 1.2	4.7 ± 1.2	3.0 ± 1.1
0.86 - 0.84	7.5 ± 1.4	13.0 ± 2.8	14.4 ± 2.8	4.9 ± 1.2	5.8 ± 1.7	3.9 ± 1.1	3.5 ± 1.1	0.9 ± 0.6
0.84 - 0.82	7.0 ± 1.5	4.8 ± 1.6	4.3 ± 1.4	3.9 ± 1.1	3.1 ± 1.0	0.5 ± 0.4	1.1 ± 0.6	1.1 ± 0.6
0.82 - 0.80	4.8 ± 1.2	3.9 ± 1.3	3.4 ± 1.2	4.4 ± 1.3	2.5 ± 0.9	2.4 ± 1.0	1.9 ± 0.8	0.5 ± 0.5
0.80 - 0.78	4.8 ± 1.2	1.7 ± 1.0	2.2 ± 1.0	1.2 ± 0.6	0.9 ± 0.5	1.4 ± 0.7	0.4 ± 0.4	0.6 ± 0.6
0.78 - 0.76	3.8 ± 1.1	2.6 ± 1.2	1.4 ± 0.8	1.3 ± 0.6	0.3 ± 0.3			
0.76 - 0.74	2.0 ± 0.8	3.5 ± 1.3	0.6 ± 0.6	0.7 ± 0.4	0.3 ± 0.3			
0.74 - 0.72	0.8 ± 0.5	0.5 ± 0.5		0.4 ± 0.4				
0.72 - 0.70	0.5 ± 0.4	0.9 ± 0.6		0.5 ± 0.4				
0.70 - 0.68	1.0 ± 0.6	0.4 ± 0.4	1.2 ± 0.7					
0.68 - 0.66	1.2 ± 0.6		0.7 ± 0.5					
σ_{tot} mb a)	7.35 ± 0.30	7.66 ± 0.43	9.04 ± 0.42	8.76 ± 0.36	8.80 ± 0.38	8.59 ± 0.40	7.18 ± 0.36	6.13 ± 0.38

a) The total cross section was obtained by a polynomial fit using the optical point.

Table 6

Differential cross section of the reaction $K^-d \rightarrow K^-pn$ at various nominal momenta of the incident K^- obtained with visible spectator.

$2\pi \frac{d\sigma}{d\Omega}$ (mb/sr) ($K^-n \rightarrow K^-n$)

cos θ \ Momentum (MeV/c)	0.620	0.660	0.700	0.740	0.780	0.820	0.860	0.900	0.940	0.980	1.020	1.060	1.100	1.140	1.180
-1.0	8.32	3.07	3.53	7.50	9.80	11.82	7.84	17.81	23.78	22.05	12.02	10.52	11.53	12.80	10.40
-0.8	±2.39	1.15	1.21	1.50	1.63	1.87	1.45	1.95	2.31	2.30	1.82	1.92	2.02	2.36	2.62
-0.8	1.54	2.21	4.11	3.02	3.92	9.34	4.19	7.79	10.10	7.91	5.43	8.69	10.04	2.27	8.11
-0.6	±1.05	1.01	0.92	0.97	1.21	1.49	1.04	1.44	1.53	1.34	1.35	1.75	1.83	0.99	2.13
-0.6	3.87	0.65	0.31	1.15	2.56	3.88	4.90	3.06	4.26	2.92	2.52	5.03	2.81	3.39	3.12
-0.4	±1.63	0.55	0.48	0.65	0.93	1.09	1.08	0.85	1.05	0.72	0.86	1.36	0.94	1.18	1.43
-0.4	0.71	1.34	1.31	0.42	0.38	2.68	1.72	1.48	1.94	2.66	0.09	0.26	3.43	0.00	4.03
-0.2	±0.69	0.71	0.55	0.40	0.36	0.80	0.61	0.67	0.74	0.97	0.67	0.29	1.22	0.00	1.58
-0.2	2.86	4.16	0.76	0.00	0.81	0.96	1.08	0.00	1.83	0.47	2.20	1.31	0.11	0.48	1.67
0.0	±1.36	1.03	0.50	0.00	0.50	0.54	0.53	0.42	0.85	0.74	0.95	0.84	0.87	0.85	1.41
0.0	1.81	1.19	1.65	2.47	1.56	1.32	1.64	0.00	0.82	0.76	1.04	1.10	0.00	1.74	0.00
0.2	±0.92	0.65	0.72	0.77	0.65	0.52	0.62	0.41	0.52	0.52	0.83	0.76	0.65	0.98	1.68
0.2	5.62	3.03	3.35	4.47	0.91	0.92	2.78	0.00	3.04	0.70	1.79	2.55	1.83	3.27	7.17
0.4	±1.65	1.05	1.09	1.17	0.67	0.65	0.87	0.28	0.80	0.73	1.08	1.04	1.06	1.08	2.11
0.4					4.36	3.09	5.28	7.41	4.81	6.60	5.79	5.47	7.26	11.92	14.45
0.6					± 1.08	1.09	1.17	1.29	1.03	1.44	1.38	1.32	1.64	2.03	2.96
σ [mb] a)	8.146	5.787	6.023	8.222	7.709	12.789	14.335	14.162	20.500	15.071	13.856	8.368	13.130	11.502	15.532
opt. point.	7.893	9.825	12.001	13.991	17.101	22.983	32.162	42.390	48.591	46.706	38.356	29.839	26.200	27.407	27.793

a) The total elastic cross section was obtained by a polynomial fit taking into account the optical point [8] in order to exclude the biased region at the three forward bins. Errors are mainly systematic and therefore not quoted.

Table 6a

Differential cross sections of the reaction $K^-d \to K^-pn$, for backward angles $-1.0 \leq \cos\theta \leq -0.6$, from events *with* and *without* visible spectator.

$2\pi \frac{d\sigma}{d\Omega}$ (mb/sr) ($K^-n \to K^-n$)

Momentum (MeV/c) / $\cos\theta$		0.700	0.778	0.837	0.902	0.963	1.036	1.095	1.172
-1.0	-0.9	4.51 ± 0.73	6.46 ± 0.97	12.82 ± 1.37	13.92 ± 1.21	19.01 ± 1.41	13.81 ± 1.26	12.15 ± 1.12	10.26 ± 1.25
-0.9	-0.8	5.38 ± 0.79	6.56 ± 0.97	8.98 ± 1.15	13.54 ± 1.25	17.93 ± 1.42	12.82 ± 1.19	10.63 ± 1.09	7.65 ± 1.01
-0.8	-0.7	4.17 ± 0.72	5.35 ± 0.96	6.20 ± 0.95	6.94 ± 0.87	9.66 ± 1.05	7.53 ± 0.89	6.38 ± 0.83	5.03 ± 0.83
-0.7	-0.6	2.87 ± 0.68	3.57 ± 1.08	4.94 ± 1.16	7.68 ± 1.28	7.45 ± 1.41	6.20 ± 1.39	3.10 ± 1.03	3.77 ± 1.54

Table 7

Differential cross section of the reaction $K^-d \rightarrow p\Lambda\pi^-$ at various nominal momenta of the incident K^-.

$$2\pi \frac{d\sigma}{d\Omega} \text{ (mb/sr) } (K^-n \rightarrow \Lambda\pi^-)$$

cos θ		Momentum (MeV/c)	700	739	778	807	837	869	902	932	963	999	1036	1065	1095	1133	1172	1212
-1.0	-0.9		4.38	4.84	4.43	10.67	7.78	5.00	8.59	5.54	5.04	3.48	1.33	0.78	1.53	0.59	0.24	1.77
		±	0.98	1.14	1.11	1.83	1.42	1.04	1.33	1.09	0.97	0.80	0.50	0.39	0.54	0.34	0.24	0.88
-0.9	-0.8		5.10	5.66	4.99	5.02	3.94	7.08	4.78	4.57	2.40	3.53	2.47	1.54	1.73	1.71	0.23	0.00
		±	1.09	1.23	1.21	1.25	0.98	1.27	0.98	0.97	0.67	0.81	0.69	0.54	0.58	0.65	0.23	0.00
-0.8	-0.7		4.04	6.67	2.91	3.31	3.74	5.02	2.52	3.63	4.05	3.18	1.51	1.53	0.53	2.15	0.02	0.00
		±	0.95	1.36	0.92	1.00	0.97	1.07	0.70	0.88	0.88	0.77	0.53	0.54	0.31	0.68	0.00	0.00
-0.7	-0.6		3.41	4.45	1.90	4.20	3.59	1.52	4.01	2.06	3.51	3.27	1.53	0.76	1.37	1.25	1.07	0.01
		±	0.88	1.11	0.72	1.12	0.96	0.58	0.90	0.65	0.81	0.77	0.54	0.38	0.52	0.51	0.54	0.00
-0.6	-0.5		1.80	2.70	2.51	5.28	2.41	4.26	2.96	1.74	2.48	2.01	1.78	0.86	1.20	1.47	0.53	0.80
		±	0.63	0.85	0.84	1.28	0.80	0.98	0.76	0.61	0.69	0.61	0.59	0.43	0.49	0.56	0.38	0.56
-0.5	-0.4		1.60	1.89	2.35	1.46	1.26	1.54	1.95	2.47	0.73	1.84	0.56	0.20	0.76	0.46	0.52	0.37
		±	0.61	0.71	0.83	0.65	0.56	0.58	0.62	0.71	0.36	0.58	0.32	0.20	0.38	0.33	0.37	0.37
-0.4	-0.3		1.59	1.67	1.40	1.83	2.29	2.94	1.78	1.65	2.61	1.05	0.38	1.01	1.22	0.42	0.00	0.00
		±	0.60	0.68	0.63	0.75	0.76	0.82	0.59	0.58	0.70	0.43	0.27	0.45	0.50	0.29	0.00	0.00
-0.3	-0.2		2.58	1.07	1.36	0.92	2.80	2.45	2.99	2.08	1.81	1.27	1.12	1.86	0.39	0.42	0.53	0.81
		±	0.78	0.53	0.61	0.53	0.84	0.74	0.77	0.66	0.57	0.48	0.46	0.62	0.27	0.30	0.37	0.57
-0.2	0.1		1.43	1.08	0.84	1.17	1.27	0.65	1.79	2.53	2.20	1.62	0.37	0.17	0.59	0.41	0.00	0.00
		±	0.59	0.54	0.48	0.58	0.57	0.38	0.60	0.73	0.63	0.54	0.26	0.17	0.34	0.29	0.00	0.00

Table 7 (continued)

cos θ \ Momentum (MeV/c)		700	739	778	807	837	869	902	932	963	999	1036	1065	1095	1133	1172	1212
-0.1	0.0	0.68	0.54	0.26	0.58	0.48	0.87	0.98	2.76	1.85	2.15	1.70	0.59	0.59	1.04	0.85	0.40
		± 0.39	0.38	0.26	0.41	0.34	0.43	0.44	0.76	0.58	0.62	0.57	0.34	0.34	0.47	0.49	0.40
0.0	0.1	0.20	0.52	1.10	0.00	1.27	0.65	0.99	1.23	2.50	1.22	1.33	0.99	1.59	0.63	0.79	0.76
		± 0.20	0.37	0.55	0.00	0.57	0.37	0.44	0.50	0.69	0.46	0.50	0.44	0.56	0.37	0.46	0.53
0.1	0.2	0.90	0.00	1.45	0.26	0.74	0.92	1.24	1.48	2.24	1.44	1.90	0.81	1.14	1.48	1.62	0.37
		± 0.45	0.00	0.65	0.26	0.43	0.46	0.51	0.56	0.65	0.51	0.60	0.41	0.46	0.56	0.66	0.37
0.2	0.3	0.72	0.25	0.57	0.26	0.72	0.64	1.00	1.70	1.30	0.86	3.22	1.21	1.97	0.60	1.90	1.14
		± 0.42	0.25	0.40	0.26	0.41	0.37	0.45	0.60	0.49	0.38	0.78	0.49	0.62	0.35	0.72	0.66
0.3	0.4	1.17	1.39	1.13	0.89	0.45	1.12	1.00	0.80	2.09	2.75	2.56	2.08	2.19	1.28	1.05	1.60
		± 0.52	0.62	0.56	0.52	0.32	0.50	0.45	0.40	0.63	0.71	0.71	0.66	0.66	0.52	0.53	0.80
0.4	0.5	0.68	1.97	2.16	0.92	0.74	0.17	2.05	1.03	2.93	3.15	2.09	2.68	2.36	3.06	1.66	1.67
		± 0.39	0.75	0.81	0.53	0.43	0.17	0.65	0.46	0.76	0.76	0.63	0.74	0.68	0.82	0.68	0.84
0.5	0.6	1.80	2.29	3.04	2.21	1.54	1.08	1.46	1.48	1.76	3.18	1.35	2.74	2.01	3.80	1.67	3.19
		± 0.68	0.81	0.96	0.84	0.63	0.48	0.55	0.56	0.59	0.77	0.51	0.76	0.64	0.92	0.68	1.13
0.6	0.7	3.07	4.75	2.62	3.46	3.21	1.16	3.56	2.19	2.56	3.94	3.16	2.96	2.69	3.85	2.18	4.22
		± 0.89	1.19	0.92	1.09	0.93	0.52	0.86	0.69	0.71	0.86	0.79	0.79	0.75	0.93	0.77	1.33
0.7	0.8	4.81	5.10	4.35	3.37	2.96	4.80	3.96	4.04	3.42	2.38	3.98	2.16	2.77	3.30	2.30	4.50
		± 1.13	1.27	1.16	1.07	0.89	1.10	0.93	0.95	0.83	0.69	0.89	0.68	0.77	0.88	0.81	1.36
0.8	0.9	3.80	4.88	6.14	6.72	4.89	5.25	6.18	3.19	4.28	3.78	5.13	2.86	2.61	1.90	3.05	0.00
		± 1.05	1.35	1.41	1.58	1.26	1.17	1.19	0.85	0.96	0.89	1.05	0.79	0.75	0.67	0.96	0.00
0.9	1.0	6.86	6.97	9.99	5.82	7.10	7.00	5.32	4.39	5.39	2.73	2.57	1.84	0.66	2.58	1.31	1.34
		± 1.53	1.64	2.04	1.68	1.59	1.61	1.29	1.10	1.15	0.82	0.81	0.65	0.38	0.86	0.65	0.77
σ[mb]		5.06	5.87	5.55	5.83	5.32	5.41	5.91	5.06	5.51	4.88	4.00	2.96	2.99	3.24	2.15	2.29
Δσ		± 0.36	0.42	0.42	0.44	0.38	0.36	0.35	0.33	0.33	0.30	0.28	0.25	0.24	0.27	0.24	0.31
No. of events		203.00	198.00	178.00	177.00	196.00	224.00	279.00	233.00	282.00	259.00	202.00	143.00	149.00	144.00	77.00	56.00

Table 8

Differential cross section of the reaction $K^-d \to p\Sigma^0\pi^-$ at various nominal momenta of the incident K^- obtained with visible spectator.

$$2\pi \frac{d\sigma}{d\Omega} \text{ (mb/sr) } (K^-n \to \Sigma^0\pi^-)$$

cos θ \ Momentum (MeV/c)		700	739	778	807	837	869	902	932	963	999	1036	1065	1095	1133	1172	1212
-1.0	-0.8	2.16	1.46	2.72	2.16	0.83	1.64	0.81	0.37	0.65	0.30	0.41	1.00	1.44	0.46	0.00	1.36
		± 1.08	0.73	1.11	1.08	0.59	0.82	0.58	0.37	0.46	0.30	0.41	0.71	0.83	0.46	0.00	0.96
-0.8	-0.6	0.00	1.92	1.70	1.05	0.00	0.94	1.63	0.89	0.32	0.60	0.89	0.00	0.00	0.00	0.00	0.52
		± 0.00	0.86	0.85	0.74	0.00	0.67	0.81	0.63	0.32	0.42	0.63	0.00	0.00	0.00	0.00	0.52
-0.6	-0.4	0.00	0.00	0.89	0.49	1.24	0.82	1.12	0.80	0.35	1.00	0.00	0.47	0.00	0.53	0.00	0.00
		± 0.00	0.00	0.63	0.49	0.72	0.58	0.65	0.57	0.35	0.58	0.00	0.47	0.00	0.53	0.00	0.00
-0.4	-0.2	1.15	0.00	0.82	0.00	0.46	0.00	0.78	0.42	0.65	0.67	0.00	0.00	0.00	0.00	0.00	0.00
		± 0.81	0.00	0.58	0.00	0.46	0.00	0.55	0.42	0.46	0.48	0.00	0.00	0.00	0.00	0.00	0.00
-0.2	0.0	0.00	0.38	0.00	0.00	0.44	0.00	0.00	0.00	0.00	0.32	0.00	0.95	0.00	0.00	0.00	0.00
		± 0.00	0.38	0.00	0.00	0.44	0.00	0.00	0.00	0.00	0.32	0.00	0.67	0.00	0.00	0.00	0.00
0.0	0.2	0.00	1.11	0.45	1.10	0.00	0.00	0.00	0.00	1.34	0.00	1.21	0.00	0.49	0.99	0.00	1.63
		± 0.00	0.64	0.45	0.77	0.00	0.00	0.00	0.00	0.67	0.00	0.70	0.00	0.49	0.70	0.00	0.94
0.2	0.4	0.00	0.39	0.88	0.58	0.89	1.27	0.00	0.41	0.33	0.00	0.00	0.49	0.50	1.40	0.58	1.15
		± 0.00	0.39	0.62	0.58	0.63	0.73	0.00	0.41	0.33	0.00	0.00	0.49	0.50	0.81	0.58	0.81
0.4	0.6	0.66	2.05	1.76	1.08	0.43	2.15	0.77	0.00	1.00	0.34	1.26	0.47	0.49	0.50	0.58	0.00
		± 0.66	0.92	0.88	0.76	0.43	0.96	0.55	0.00	0.58	0.34	0.73	0.47	0.49	0.50	0.58	0.00
0.6	0.8	2.84	0.78	0.43	3.37	0.00	0.43	0.77	0.97	1.00	1.06	0.86	1.10	0.00	0.50	1.17	0.00
		± 1.27	0.55	0.43	1.38	0.00	0.43	0.55	0.69	0.58	0.61	0.61	0.78	0.00	0.50	0.82	0.00
0.8	1.0	2.64	2.51	2.27	1.21	1.89	0.45	0.00	1.46	0.71	0.39	2.64	0.00	0.73	1.67	0.82	0.62
		± 1.32	1.25	1.01	0.85	0.94	0.45	0.00	0.84	0.50	0.39	1.32	0.00	0.73	0.96	0.82	0.62
σ[mb]		1.89	2.12	2.38	2.21	1.24	1.54	1.18	1.06	1.27	0.94	1.46	0.90	0.73	1.21	0.63	1.06
Δσ		0.47	0.42	0.46	0.49	0.33	0.36	0.30	0.31	0.29	0.25	0.38	0.30	0.28	0.35	0.28	0.35
No. of events		16.00	25.00	27.00	20.00	14.00	18.00	15.00	12.00	19.00	14.00	15.00	9.00	7.00	12.00	5.00	9.00

Table 9

Differential cross section of the reaction $K^-d \to p\Sigma^-\pi^0$ at various nominal momenta of the incident K^- obtained with visible spectator.

$$2\pi \frac{d\sigma}{d\Omega} \text{ (mb/sr)} \quad (K^-n \to \Sigma^-\pi^0)$$

cos θ \ Momentum (MeV/c)		700	739	778	807	837	869	902	932	963	999	1036	1065	1095	1133	1172	1212
-1.0	-0.8	1.37	1.30	2.16	0.46	0.00	1.75	0.66	1.72	1.09	0.27	1.69	0.39	1.20	1.16	0.48	0.00
		± 0.79	0.65	0.88	0.46	0.00	0.78	0.47	0.77	0.55	0.27	0.76	0.39	0.69	0.67	0.48	0.00
-0.8	-0.6	1.36	2.33	2.64	0.91	1.11	0.72	0.31	0.66	0.27	0.56	0.35	0.40	0.00	0.77	1.42	0.45
		± 0.79	0.88	1.00	0.64	0.64	0.51	0.31	0.47	0.27	0.40	0.35	0.40	0.00	0.55	0.82	0.45
-0.6	-0.4	2.77	1.31	0.73	0.00	0.41	1.44	0.33	0.00	0.00	0.00	0.32	0.00	0.43	1.20	0.00	0.00
		± 1.13	0.66	0.52	0.00	0.41	0.72	0.33	0.00	0.00	0.00	0.32	0.00	0.43	0.69	0.00	0.00
-0.4	-0.2	1.88	0.63	0.37	0.00	0.39	0.00	0.34	0.00	0.29	0.27	0.00	0.00	0.39	0.00	0.00	0.00
		± 0.94	0.45	0.37	0.00	0.39	0.00	0.34	0.00	0.29	0.27	0.00	0.00	0.39	0.00	0.00	0.00
-0.2	0.0	0.00	0.00	0.00	0.45	0.40	0.40	0.34	0.39	0.28	0.26	0.00	0.00	0.44	0.41	0.49	0.00
		± 0.00	0.00	0.00	0.45	0.40	0.40	0.34	0.39	0.28	0.26	0.00	0.00	0.44	0.41	0.49	0.00
0.0	0.2	0.49	0.35	0.00	0.00	0.76	0.00	0.34	0.74	0.88	0.30	1.39	0.41	0.00	0.40	0.00	0.48
		± 0.49	0.35	0.00	0.00	0.54	0.00	0.34	0.52	0.51	0.30	0.70	0.41	0.00	0.40	0.00	0.48
0.2	0.4	0.00	0.77	0.37	1.89	0.00	0.79	0.35	0.35	0.90	1.78	0.71	0.82	1.29	0.41	1.03	0.47
		± 0.00	0.54	0.37	0.95	0.00	0.56	0.35	0.35	0.52	0.73	0.50	0.58	0.74	0.41	0.73	0.47
0.4	0.6	1.07	1.10	1.71	2.76	0.76	1.60	0.33	0.71	0.28	1.57	0.00	0.86	2.18	0.46	1.07	0.50
		± 0.76	0.63	0.86	1.24	0.54	0.80	0.33	0.50	0.28	0.70	0.00	0.61	0.98	0.46	0.75	0.50
0.6	0.8	1.05	1.65	1.66	2.06	0.89	1.55	1.06	0.00	0.32	0.62	1.20	0.53	0.60	0.47	0.59	1.21
		± 0.74	0.83	0.83	1.03	0.63	0.78	0.61	0.00	0.32	0.44	0.69	0.53	0.00	0.47	0.59	0.86
0.8	1.0	3.01	1.80	1.79	3.73	1.57	1.75	0.83	1.19	0.32	0.67	0.00	0.00	0.00	0.00	1.31	0.00
		± 1.35	0.90	0.89	1.52	0.91	0.88	0.58	0.69	0.32	0.47	0.00	0.00	0.00	0.00	0.93	0.00
σ[mb]		2.60	2.25	2.28	2.46	1.25	2.00	0.98	1.15	0.93	1.26	1.13	0.68	1.18	1.06	1.28	0.62
Δσ		0.51	0.40	0.42	0.51	0.32	0.39	0.26	0.29	0.23	0.28	0.28	0.24	0.32	0.29	0.37	0.25
No. of events		26.00	31.00	29.00	23.00	15.00	26.00	14.00	16.00	16.00	21.00	16.00	8.00	14.00	13.00	12.00	6.00

Table 10
Polarisation of the Λ in the reaction $K^-d \to p\Lambda\pi^-$.

cos θ \ Momentum (MeV/c)	700	739	778	807	837	869	902	932	963	999	1036	1065	1095	1133	1172	1212
-1.0 -0.8	0.22	0.18	0.94	0.70	0.64	-0.23	0.25	-0.36	0.38	-0.53	0.14	0.69	-0.83	0.78	-2.08	0.86
	±0.42	0.49	0.49	0.41	0.43	0.39	0.32	0.45	0.43	0.47	0.58	0.45	0.75	0.70	2.57	1.23
-0.8 -0.6	1.35	0.07	1.65	-0.05	0.36	0.34	-0.92	0.46	0.50	0.33	0.84	0.30	0.47	0.32	1.31	0.86
	±0.47	0.46	1.06	0.50	0.55	0.49	0.46	0.47	0.46	0.49	0.61	0.70	0.98	0.69	1.34	0.00
-0.6 -0.4	0.05	0.75	-1.05	2.20	0.30	0.59	0.27	-0.05	0.47	-0.11	-0.20	-0.84	-0.92	1.73	0.83	-0.79
	±0.79	0.64	0.78	0.77	0.61	0.47	0.54	0.54	0.70	0.56	0.82	1.11	1.03	0.93	1.80	1.58
-0.4 -0.2	-0.59	0.28	1.28	0.38	-1.45	-0.57	0.52	0.50	1.08	0.28	1.33	-0.83	-0.29	0.73	2.54	2.21
	±0.74	0.95	0.95	0.86	0.55	0.68	0.59	0.63	0.61	0.71	0.89	0.64	0.88	1.51	1.80	1.57
-0.2 0.0	-1.66	0.43	-0.36	1.03	0.04	-1.30	0.63	0.35	-0.67	0.40	0.06	1.99	-1.32	2.08	1.70	-0.60
	±0.94	1.30	1.86	1.27	1.43	1.26	0.70	0.49	0.54	0.53	0.73	1.41	1.48	1.21	1.31	0.60
0.0 0.2	0.68	1.56	-1.20	-0.53	1.37	-1.17	0.03	0.70	1.13	1.10	0.53	2.64	0.55	-0.18	-0.74	1.55
	±1.00	1.63	0.80	0.53	0.97	0.71	0.77	0.76	0.52	0.81	0.71	0.95	0.70	1.09	0.90	0.99
0.2 0.4	1.03	-1.12	-2.04	-3.40	-1.20	0.01	-0.59	2.60	-0.61	0.47	0.35	0.91	1.38	0.04	0.74	1.49
	±1.21	1.16	1.44	2.02	1.12	1.16	0.60	0.91	0.64	0.62	0.47	0.86	0.70	1.09	1.02	0.99
0.4 0.6	-0.94	-0.57	-1.42	-0.01	0.26	-2.10	1.53	0.15	-0.29	0.48	-0.29	-0.28	-0.41	-0.24	0.48	-0.82
	±0.91	0.93	0.66	0.90	0.88	1.71	0.72	0.94	0.60	0.43	0.65	0.56	0.62	0.49	0.76	1.19
0.6 0.8	0.26	-1.46	-0.25	-0.44	-0.37	-0.19	-0.53	-0.62	-1.21	-0.83	-0.44	-0.97	-0.52	0.29	-0.04	-0.64
	±0.51	0.47	0.52	0.68	0.57	0.58	0.52	0.50	0.48	0.48	0.46	0.61	0.57	0.54	0.50	0.73
0.8 1.0	-0.42	-0.27	-0.28	-0.04	-0.06	0.35	0.19	-0.50	-1.01	-1.34	-0.81	-0.80	0.09	-0.73	-0.39	0.57
	±0.51	0.43	0.46	0.48	0.55	0.47	0.50	0.52	0.43	0.51	0.43	0.60	0.88	0.62	0.71	1.84

cally lower for the neutron reaction; this is some measure of the accuracy obtainable in deuterium experiments.

3.5. *Results.*

Table 2 gives the cross section of K^-d interactions for different beam momenta p_K. Except for the elastic scattering on the deuteron $K^-d \rightarrow K^-d$, these cross sections do not correspond to a unique CM energy, but are folded with the Hulthén function. Therefore their physical meaning is limited and the values are mainly of practical importance.

Table 3 gives K^-n cross sections for eight different equivalent beam momenta corresponding to a certain (K^-n) mass. The normalisation has been obtained relative to the $\Lambda\pi$ final state, as described above in subsect. 3.4.

Table 4 gives the K^-n cross sections for some predominant two-body final states with absolute normalisation by τ-decays (subsect. 3.2). A Glauber correction of approximately 7% was applied. We note that we cannot obtain the K^-n total cross section by a straight-forward summation of all partial cross sections, as it is possible in K^-p interactions. This is due to the interference between K^-n and K^-p states in the elastic channels. Their separation is always model dependent.

Tables 5 to 9 give differential cross sections $2\pi\, d\sigma/d\Omega$ for reactions $K^-d \rightarrow K^-d$, $K^-n \rightarrow K^-n$, $\Lambda\pi^-$, $\Sigma^0\pi^-$, $\Sigma^-\pi^0$. The scattering angle θ is defined as

$$\cos\theta = \frac{\boldsymbol{p}_K \cdot \boldsymbol{p}_{meson}}{|\boldsymbol{p}_K| \cdot |\boldsymbol{p}_{meson}|}$$

in the K^-n system (or in the K^-d system for K^-d scattering). Finally, table 10 gives the polarization P of the Λ in reaction $K^-n \rightarrow \Lambda\pi^-$ which was determined from

$$\alpha P(\cos\theta) = \frac{3\Sigma \cos\xi}{N} \pm \sqrt{\frac{3 - (\alpha P)^2}{N}},$$

with

$$\cos\xi = \frac{(\boldsymbol{p}_K \times \boldsymbol{p}_\pi) \cdot \boldsymbol{p}_p}{|\boldsymbol{p}_K \times \boldsymbol{p}_\pi| \, |\boldsymbol{p}_p|}$$

and $\alpha = 0.65$, N the number of events, and $\boldsymbol{p}_K$, $\boldsymbol{p}_\pi$ and $\boldsymbol{p}_p$ the momentum vectors of the incoming K^-, the produced pion and the decay proton in the Λ rest frame.

3.6. *The total elastic cross section.*

The direct determination of the K^-n elastic cross section suffers from the technical biases in the analysis of the two-prong reactions (subsect. 2.4) and from its indistinguishability from K^-p interactions for small momentum transfers.

In principe we can derive, however, the total elastic K^-n cross section by a substraction procedure from the K^-n total cross section [8],

Table 11
Total elastic K^-n cross section as obtained by subtraction from the total K^-n cross section.

P_K (MeV/c)	σ_{tot} (mb)[8]	$\sigma_{reaction}$ (mb)	σ_{el} (mb)
702	27.0 ± 0.5	14.1 ± 1.6	12.9 ± 1.7
778	29.2 ± 0.5	14.3 ± 0.8	14.9 ± 1.0
837	34.0 ± 0.5	15.3 ± 0.8	18.7 ± 1.0
903	39.0 ± 0.5	19.7 ± 1.1	19.3 ± 1.2
963	40.5 ± 0.5	20.5 ± 0.9	20.0 ± 1.0
1034	37.0 ± 0.5	19.9 ± 1.2	17.1 ± 1.3
1098	31.8 ± 0.5	18.4 ± 1.0	13.4 ± 1.1
1173	29.0 ± 0.5	16.5 ± 1.3	12.5 ± 1.4

$$\sigma_{total} = \sigma_{elastic} + \sigma_{reaction} ,$$

where $\sigma_{reaction}$ is obtained using all inelastic events N_r and normalizing by the method described in subsect. 3.4.

$$\sigma_{reaction} = 2\sigma(\Lambda\pi^0) \frac{N_{reaction}}{1.5\, N(\Lambda\pi^-)} ,$$

$$\sigma_{elastic} = \sigma_{total} - 2\sigma(\Lambda\pi^0) \frac{N_{reaction}}{1.5\, N(\Lambda\pi^-)} .$$

The result is given in table 11.

We thank our scanning and measuring staff for their collaborative efforts.

REFERENCES

[1] R. Armenteros, M. Ferro-Luzzi, D. W. G. S. Leith, R. Levi-Setti, A. Minten, R. Tripp, H. Filthuth, V. Hepp, E. Kluge, H. Schneider, R. Barloutaud, P. Granet, J. Meyer and J. P. Porte, Nucl. Phys. B8 (1968) 233.
[2] J. Duboc, A. Minten and S. G. Wojcicki; CERN 65-2 (1965).
[3] R. B. Bell, R. W. Birge, Yu-Li Pan and R. T. Pu, Phys. Rev. Letters 16 (1966) 203;
W. M. Smart, A. Kernan, G. E. Kalmus and R. P. Ely Jr., Phys. Rev. Letters 17 (1966) 556;
A. Kernan and W. M. Smart, Phys. Rev. Letters 17 (1967) 832;
R. B. Bell, Phys. Rev. Letters 19 (1967) 936;
D. Cline and M. G. Olsson, Phys. Letters 25B (1967) 41;
W. H. Sims, J. R. Albright, E. B. Brucker, J. T. Dockery, J. E. Lannutti, J. S. O'Neall, B. G. Reynolds, J. H. Bartley, R. M. Dowd, A. F. Greene, J. Schneps, M. Meer, J. Mueller, M. Schneeberger and S. Wolf, Phys. Rev. Letters 21 (1968) 1413.
[4] R. Armenteros, P. Baillon, C. Bricman, M. Ferro-Luzzi, H. K. Nguyen, V. Pelosi, D. E. Plane, N. Schmitz, E. Burkhardt, H. Filthuth, E. Kluge, H. Oberlack, R. R. Ross, R. Barloutaud, P. Granet, J. Meyer, J. L. Narjoux, F. Pierre, J. P. Porte and J. Prevost, Nucl. Phys. B8 (1968) 183, 216;
R. Armenteros, P. Baillon, A. Minten, Nguyen H. Khanh, V. Pelosi, M. Crozon, C. Louedec, J. L. Narjoux and F. Pierre, Nucl. Phys. B10 (1969) 459;

J. Meyer, Proc. Heidelberg Int. Conf. on elementary particles (North Holland, 1967) p.117.
[5] L. Hulthén and M. Sugawara, Handbuch der Physik, Vol XXXIX (Springer Verlag 1957).
[6] M. J. Moravcsik, Nucl. Phys. 7 (1958) 113.
[7] R. J. Glauber, High energy physics and nuclear structure (North Holland, 1967).
[8] D. V. Bugg, R. S. Gilmore, K. M. Knight, D. C. Salter, G. H. Stafford, E. J. N. Wilson, J. D. Davies, J. D. Dowell, P. M. Hattersley, R. J. Homer, A. W. O'Dell, A. A. Carter, R. J. Tapper and K. F. Riley, Phys. Rev. 168 (1968) 1466.